

Pacific Ocean wind stress and surface heat flux anomalies from NCEP reanalysis and observations: Cross-statistics and ocean model responses

Guillermo Auad, Arthur J. Miller, John O. Roads, and Daniel Cayan¹

Scripps Institution of Oceanography, La Jolla, California

Abstract.

Wind stresses and surface heat fluxes over the Pacific Ocean from the National Center for Environmental Prediction (NCEP) reanalysis and the comprehensive Ocean-Atmosphere Data Set (COADS) (blended with FSU tropical wind stresses) are compared over a common time interval (1958–1997) in their statistics and in the responses that they induce in sea surface temperature (SST) and heat storage when used to force an ocean model. Wind stress anomalies from the two data sets are well correlated in the midlatitude extratropics, especially in the highly sampled North Pacific. In the tropics and subtropics, low correlations were found between the two wind stress data sets. The amplitudes of the stress variations of the two data sets are similar in midlatitudes, but in the tropics NCEP wind stresses are weaker than the COADS/FSU stresses, especially on interannual timescales. Surface heat flux anomalies from the two data sets are well correlated on interannual and shorter timescales in the North Pacific Ocean poleward of 20°N, but they are poorly correlated elsewhere and on decadal timescales. In the extratropics the amplitudes of the heat flux variations of the two data sets are comparable, but in the tropics the NCEP heat fluxes are weaker than those of COADS. Ocean model hindcasts driven by both data sets are also compared. The midlatitude SST hindcasts were superior when using the NCEP flux anomalies while tropical SST hindcasts were equally skillful for the two hindcasts when considering all climatic timescales. The spatial and temporal sampling rates of the COADS observations and their consequent impacts on constraining the NCEP reanalysis appear to be the main factors controlling the results found here.

1. Introduction

Wind stress and surface heat flux fields over the ocean are often used for diagnosing ocean-atmosphere climate variations [e.g., *Cayan*, 1992b; *Trenberth and Hurrel*, 1994; *Iwasaka and Wallace*, 1995; *Tanimoto et al.*, 1997; *Deser et al.*, 1999; *Parrish et al.*, 2000] and for forcing and testing numerical models of ocean climate variations [e.g., *Harrison et al.*, 1990; *Miller et al.*, 1993, 1994; *Xie et al.*, 2000; *Stockdale et al.*, 1998; *Fevrier et al.*, 2000].

Surface heat and momentum fluxes derived from direct observations, however, are usually sparsely sampled in space and time, especially in tropical, subtropical, and Southern Hemisphere regions. These surface flux estimates are also infected by uncertainties in the bulk formulae [*Blanc*, 1985; *Weare*, 1989; *Taylor*, 1984] and by errors in the weather observations [e.g., *Ram-*

age, 1984, 1987; *Barnett*, 1984; *Wright*, 1986; *Morrissey*, 1990; *Cayan*, 1992a; *Ward and Hoskins*, 1996] that are employed in deriving the fluxes. The portion of the observational error that is random may be reduced by aggregating over multiple flux estimates in time and space so that well-sampled areas of the ocean, e.g., parts of the North Pacific and North Atlantic Oceans, have more reliable flux estimates than those that are poorly sampled, e.g., much of the tropics and Southern Ocean [*Weare*, 1989; *Cayan*, 1992a]. More difficult problems are those that produce constant or time-varying biases, caused by uncertainties in the bulk formulae and by instrumental practices such as changes in surface wind estimation procedures or by increases in ship anemometer height [*Taylor*, 1984].

Atmospheric analyses can provide relatively complete spatial and temporal coverage but they can be influenced by model errors [*Betts et al.*, 1996; *Weare*, 1997; *Bony et al.*, 1997; *Trenberth and Guillemot*, 1998; *Scott and Alexander*, 1999; *Yang et al.*, 1999], by inadequate quantities of assimilated data [*Waliser et al.*, 1999; *Marshall and Harangozo*, 2000; *Putman et al.*, 2000],

This paper is not subject to U.S. copyright. Published in 2001 by the American Geophysical Union.

Paper number 2000JC000264.

and by the exclusion of data that are difficult to assimilate such as surface heat fluxes and rainfall [Janowiak *et al.*, 1998].

In recent years, surface fluxes from the National Centers for Environmental Prediction/National Center for Atmospheric Research (NCEP/NCAR) reanalysis have become routinely available [Kalnay *et al.* 1996]. Surface fluxes derived from direct observations associated with the Comprehensive Ocean-Atmosphere Data Set (COADS) are also available for a similar time period [Woodruff *et al.*, 1987; Cayan 1992a; da Silva *et al.*, 1994]. The forcing functions derived from these two sources are ubiquitously being used to force ocean models for simulating and diagnosing observed basin-scale ocean climate variations over long timescales.

These ocean hindcasts have revealed numerous aspects of the physics of oceanic climate variations on seasonal to interannual and decadal timescales. Tropical ocean hindcasting has revealed the sensitivity of the tropical ocean circulation to the interannual wind stress forcing and the damping effect of surface heat fluxes [e.g., Harrison *et al.*, 1990; Barnett *et al.*, 1991; Stockdale *et al.*, 1998]. In the midlatitudes, heat fluxes appear to play the major role in driving sea surface temperature anomalies (SST) anomalies on seasonal to interannual timescales [e.g., Luksch and von Storch, 1992; Miller *et al.*, 1994; Battisti *et al.*, 1995; Kleeman *et al.*, 1996; Halliwell, 1998; Giese and Carton, 1999; Seager *et al.*, 2000]. However, horizontal currents can contribute substantially to midlatitude SST evolution during certain intervals and on the longer timescales [Miller *et al.*, 1994; Giese and Carton, 1999], and especially in western boundary current regions [Kleeman *et al.*, 1996; Halliwell, 1998; Xie *et al.*, 2000; Qiu, 2000]. Subsurface midlatitude adjustment processes due to Rossby waves [e.g., Lysne *et al.* 1997; Miller *et al.*, 1997] and subduction by mean currents [Schneider *et al.*, 1999] have also been identified in these ocean climate hindcasts.

These results of driving ocean models with surface heat and momentum flux estimates, however, are impaired by inaccuracies in the fluxes as well as by inadequacies in the ocean models. The consistency of model physics can be rigorously tested using error statistics of the atmospheric forcing and of the validating oceanic data sets [e.g., Frankignoul *et al.*, 1989, 1995; Senechal *et al.*, 1994; Bennett *et al.*, 1998, 2000], but the computational requirements of such tests of full-physics models can be ominous.

Using observed flux variations to force ocean models clearly leads to a better understanding of how the ocean can interact with the atmosphere to organize climate variations. But it is unclear how the uncertainty in the flux estimates is transferred to errors in the ocean model physical balances. How similar are the COADS and NCEP flux forcing data sets which are commonly used to force ocean models? How differently would a single model respond to forcing by these two data sets? Our goal is to answer these questions as follows: We first statistically analyze the NCEP and COADS surface

flux forcing fields for the Pacific for the period 1958–1997 to determine the similarity of the two data sets over monthly, interannual, and interdecadal timescales. We also use the two data sets to provide anomalous forcing for an ocean model of the Pacific and compare the results with observations of SST and heat content. These ocean hindcasts extend the Pacific Ocean decadal processes studies of Miller *et al.* [1994, 1998], Cayan *et al.* [1995] and Auad *et al.* [1998b] to longer timescales with higher spatial resolution.

This comparison provides a general understanding of the similarities and differences of the COADS and NCEP flux data sets and the character of oceanic response to be expected when using either dataset as forcing. In summary, we find that the COADS and the NCEP reanalysis still require improvements, but that they appear to be adequate in many regions for forcing long ocean model hindcasts.

This paper is organized as follows. In section 2 we describe both surface flux data sets; in section 3, their statistics are compared; section 4 compares responses of the ocean model to forcing obtained from both data sets; section 5 contains a summary and conclusions.

2. Data Sets

The time span of the COADS [Woodruff *et al.*, 1987] studied here is from January 1951 to December 1997 in a Pacific domain from 40°S to 60°N. Figure 1 shows the global sampling density of COADS wind speed and SST measurements.

Wind stress (momentum flux) anomalies were derived from COADS on a 2° X 2° grid following Cayan [1992a]. In the extratropics the COADS wind stress anomalies are derived from monthly means of the product $|V|V$ from individual wind speed observations. Drag coefficients were taken from Isemer and Hasse [1987] and are weakly dependent upon wind speed and air-sea temperature difference, ΔT . We used this COADS analysis, rather than that of da Silva *et al.* [1994], because the unadjusted COADS observations have low frequency drifts in primary variables, such as wind speed, which are thought to be spurious effects of instrumental changes. The COADS analysis we used makes a rough attempt to correct for changes in wind speed, ΔT , and surface heat flux, ΔQ by removing basinwide low-frequency drifts from these variables before fluxes are calculated via bulk formulae (see Miller *et al.* [1994] for additional details). The da Silva *et al.* [1994] analysis does not address these time-varying problems that could have substantial impact upon modeled decadal variability.

Since the COADS wind stress observations are very lightly sampled in the low latitudes (Figure 1), we use Florida State University (FSU) subjectively analyzed wind stress anomalies [Goldenberg and O'Brien, 1981] in the region $\pm 20^{\circ}$ latitude. In an overlap region of 5° latitude at 20° N and at 20° S the COADS and FSU anomaly fields were smoothly merged. Unfortunately,

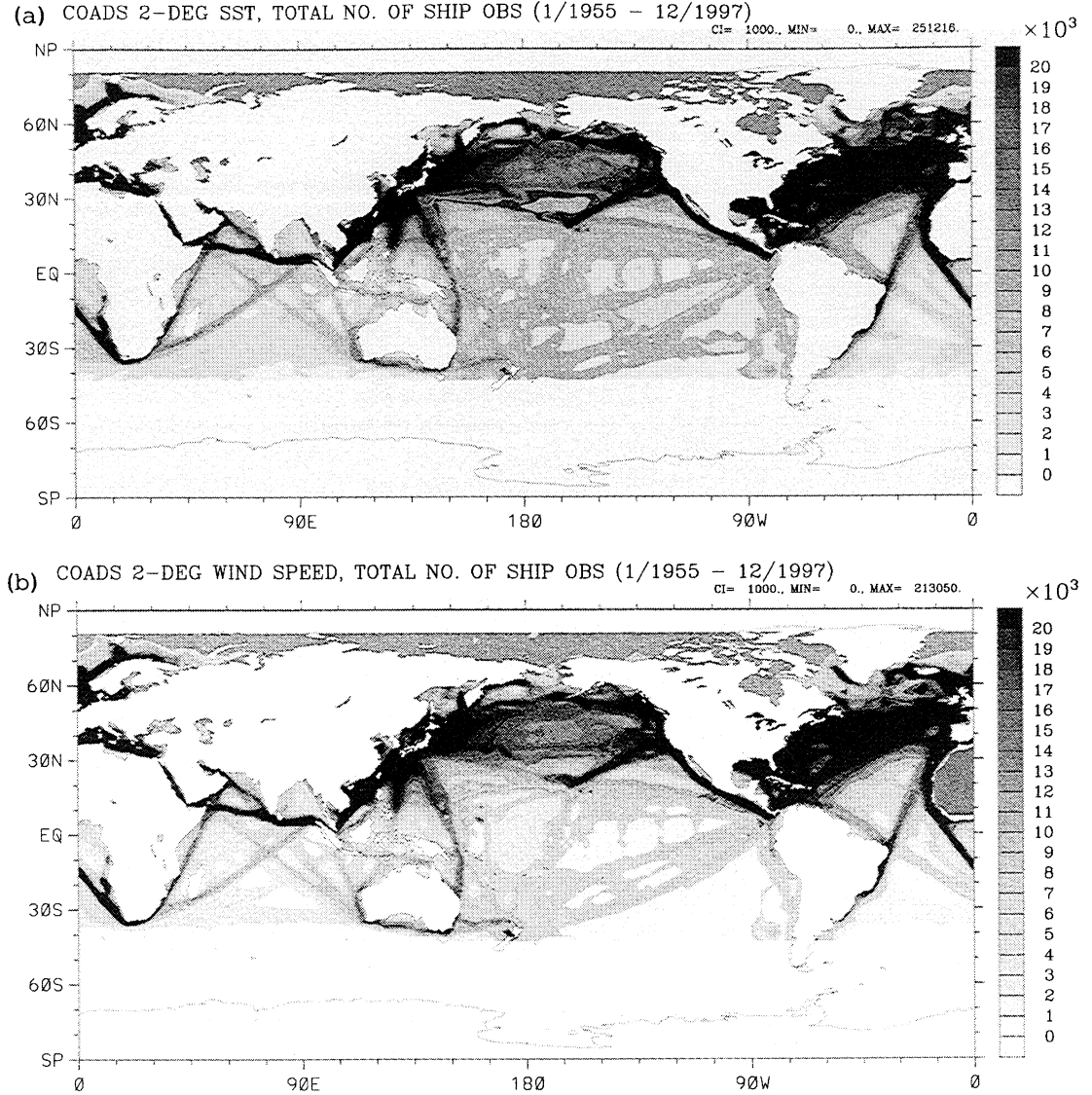


Figure 1. Distribution of the total number of observations for (top) COADS SSTs and (bottom) winds. Data plotted include observations from 1955 through 1997.

FSU winds are only available since 1961. So, we created pseudo-FSU wind stress starting in 1951 as follows. We computed empirical orthogonal functions (EOFs) of FSU wind stress from 1961 through 1997. The principal component of the first EOF was highly correlated to the Southern Oscillation Index. We regressed this index for 1951-1960 onto spatial loading pattern for EOF-1 from the period 1961-1997. We then computed the EOFs of the COADS wind stresses for the period 1951-1960 in the FSU region. The second and third COADS EOFs for 1951-1960 resemble the second and third FSU EOFs for 1961-1997. So we used the principal components of the second and third COADS EOF modes as time series for the 2nd and 3rd FSU EOF modes for the period 1951-1960. The three-EOF mode reconstruction explained about 60% of the FSU wind stress variance in the period 1961-1997. We therefore expect that the reconstruction will explain a similar amount of wind stress variance for the period 1951-1960.

Missing data values in space and time were treated as follows. We first linearly interpolated in time for those missing values which had nonmissing values available in the previous and following months. We then linearly interpolated in space for any remaining missing values which were surrounded by four grid points with non-missing values. The remaining missing values were estimated by quadratic interpolation using subroutines "blockmean" and "surface" from Generic Mapping Tools (GMT). The last step was to map all of the fields to a common grid, which for convenience was chosen to be the ocean model grid (discussed in section 4), a roughly 1.5° grid covering the Pacific Ocean from Antarctica to the Arctic.

2.1. COADS Wind Stress

Heat flux anomalies were likewise computed on a 2° by 2° grid by Cayan [1992a] for the COADS observations poleward of the 10° latitude. The convention is

that positive values correspond to heat entering the ocean. The COADS latent and sensible fluxes were formed from monthly averages of products of individual observations using bulk formulae. Exchange coefficients were taken from *Isemer and Hasse* [1987] and are weakly dependent on wind speed and ΔT . During the 1950s many observations of SST and wind speed were not accompanied by humidity measurement, and so heat fluxes were not calculated directly from bulk formulae. Instead, heat flux was determined at those points by a regression with SST and wind speed. Two sets of regression coefficients were computed, one for midlatitudes and another set for the tropics. It is important to note that in the tropical band ($\pm 10^\circ$) the COADS dataset has many gaps in space and time; for convenience these were filled in using the GMT subroutines mentioned previously.

2.2. NCEP/NCAR Reanalysis

The atmospheric reanalysis was obtained with the NCEP T62 (209 km) global spectral model of 28 vertical levels with 5 levels in the boundary layer. The NCEP reanalysis model includes parameterizations of all major physical processes, namely, convection, large scale precipitation, shallow convection, gravity wave drag, radiation with diurnal cycle and interaction with clouds, boundary layer physics, an interactive surface hydrology, and vertical and horizontal diffusion processes. The details of the model physics and dynamics are given by *Kalnay et al.* [1996].

Flux fields are derived from the four times per day near surface fields produced by NCEP's global atmospheric analyses. These fields are converted with bulk formulae using a constant drag coefficient. The data were then monthly averaged for use in comparing to COADS and in forcing the ocean model.

2.3. Turbulent Kinetic Energy

The turbulent kinetic energy (TKE) flux into the mixed layer is needed as a forcing function for the bulk mixed layer formulation of the ocean model described in section 4. The fields of TKE from COADS and NCEP will not be compared here because its estimation is very uncertain when using monthly mean observations. The Weibull parameterization of *Pavia and O'Brien* [1986] for relating mean wind speed cubed to monthly mean wind speed is invoked to estimate its variability as a forcing function for both flux data sets (see *Miller et al.* [1994] for details). The area with the largest TKE anomalies is the central North Pacific which shows an increase in its variability in the late 1970s.

3. COADS and NCEP Flux Comparisons

Our goal is to compare the two different flux data sets that are frequently used in various ocean modeling studies. It is important to note that the NCEP reanalysis assimilates COADS as well as other observations. For this reason, areas with a high density of observations will be more likely to agree. However, the fluxes were computed using different bulk formulae with different ways for estimating input variables, such as SST [*Kalnay et al.*, 1996; *Cayan*, 1992a]. Determining whether the main differences are due to the different bulk formulae used in the COADS/FSU and NCEP data sets or to the different input variable estimates employed in computing the respective heat fluxes is beyond the scope of this paper. It is important to highlight that even though the COADS and NCEP heat fluxes are computed through different formulations we want to compare them as they are, without using a common bulk formulae framework, because this is the way

ANALYZED AREAS

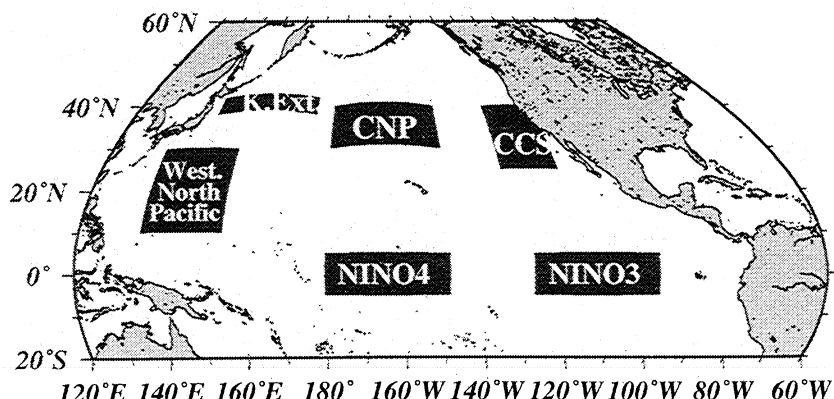


Figure 2. Key regions used in the correlation and coherence analysis in Tables 1 and 2. The “N 20°N” region in Tables 1 and 2 is the entire basin averaged north of 20°N.

Table 1. Correlations, Standard Deviations ratios, Coherence, Amplitude of Transfer Function and Lag for COADS and NCEP zonal wind stress

Area	Corr	SD	Coherence				
			2years	2.5years	3.3years	5years	10years
EEP	0.23	2.20	0.40	0.27	0.25	0.28	0.15
WEP	(0.60)	(2.83)	(0.65)	(0.84)	(0.82)	(0.85)	(0.77)
(CCS	(0.89)	(0.91)	(0.86)	(0.81)	(0.68)	(0.62)	0.55
CNP	(0.89)	(0.68)	(0.76)	(0.77)	(0.86)	(0.76)	0.55
N 20°N	(0.81)	(0.78)	(0.77)	(0.61)	(0.82)	(0.85)	(0.78)
K.Ext.	(0.87)	(0.80)	(0.65)	(0.65)	(0.78)	(0.80)	(0.69)
WNP	(0.75)	(1.31)	(0.13)	(0.38)	(0.62)	0.55	0.54

CORR and SD were computed using anomalous time series with no filtering. Results from the cross-spectral analysis are shown for the five lowest (climate) bands of the computation (2, 2.5, 3.3, 5 and 10 years). All ratios are COADS/NCEP, and a negative lag implies that NCEP leads COADS. Values in parentheses are significant at the 90% level

Amplitude					Lag (months)				
2years	2.5years	3.3years	5years	10years	2years	2.5years	3.3years	5years	10years
1.30	1.00	1.12	1.10	0.74	-1.62	-0.93	-1.06	-0.59	4.71
(1.92)	(2.05)	(1.94)	(2.00)	(1.70)	(-0.05)	(0.27)	(-0.37)	(-2.48)	(-4.00)
(0.77)	(0.64)	(0.77)	(0.65)	0.40	(0.39)	(0.29)	(0.04)	(-1.78)	-1.56
(0.70)	(0.75)	(0.78)	(0.58)	0.48	(-0.13)	(0.09)	(-0.27)	(0.20)	2.56
(0.97)	(0.82)	(0.86)	(0.83)	(0.90)	(0.01)	(-0.23)	(-0.34)	(-0.78)	(3.33)
(0.66)	(0.81)	(0.94)	(0.72)	(0.76)	(-0.25)	(0.33)	(0.04)	(0.01)	(4.25)
0.73	(0.53)	(0.73)	0.63	0.96	-1.63	(1.63)	(3.43)	5.84	4.97

in which they are presently used by the community to force ocean models. With these similarities and differences in mind, we next analyze their statistics and cross statistics to provide an a priori, general idea of how the two data sets may differ when used as oceanic forcing functions.

3.1. Wind Stress

Figure 2 shows the regions for which area-averaged time series were constructed. These areas were selected because they cover key dynamical regions of the North Pacific, most of which have been previously studied [e.g., Stockdale *et al.*, 1998; Miller *et al.*, 1994; Auad *et al.*, 1998a, 1998b].

Table 1 shows some basic statistics between NCEP and COADS/FSU zonal wind stress in these seven key regions of the equatorial and North Pacific. The meridional stress statistics show a similar level of agreement, although the phase discrepancy is much worse in the tropics.

The highest correlations and the best agreements in coherence amplitude and phase occur in the midlatitudes. In the eastern equatorial Pacific (EEP) region the correlation and coherency are weak and insignificant. In the western equatorial Pacific (WEP) region,

there is a clear disagreement in amplitude in spite of significant coherency. In the tropics, NCEP zonal wind stresses are much weaker than COADS/FSU [Putman *et al.*, 2000]. This difference decreases away from the tropics, such as in the western subtropical North Pacific area which shows a much better correspondence (Table 1).

We next discuss the spatial structure of the zero-lag correlation coefficients between NCEP and COADS/FSU wind stress anomalies. Figure 3 shows that both components of the wind stress field are well correlated north of 20°N, in contrast to low correlations, below 0.3, that occur in the tropical band. In the Southern Hemisphere the correlations increase relative to the tropics, but they reach 0.6 only in a limited area off the Australian coast.

The area displaying the lowest correlations is the eastern tropical Pacific, where wind stress variables are poorly sampled in space and time. Caution should therefore be used when interpreting these maps because a low correlation does not necessarily mean that the NCEP model is not providing a good representation of the wind field there or that the bulk formulae used to obtain the COADS/FSU data sets are unrealistic. Low correlations could simply mean inadequate sampling in COADS/FSU.

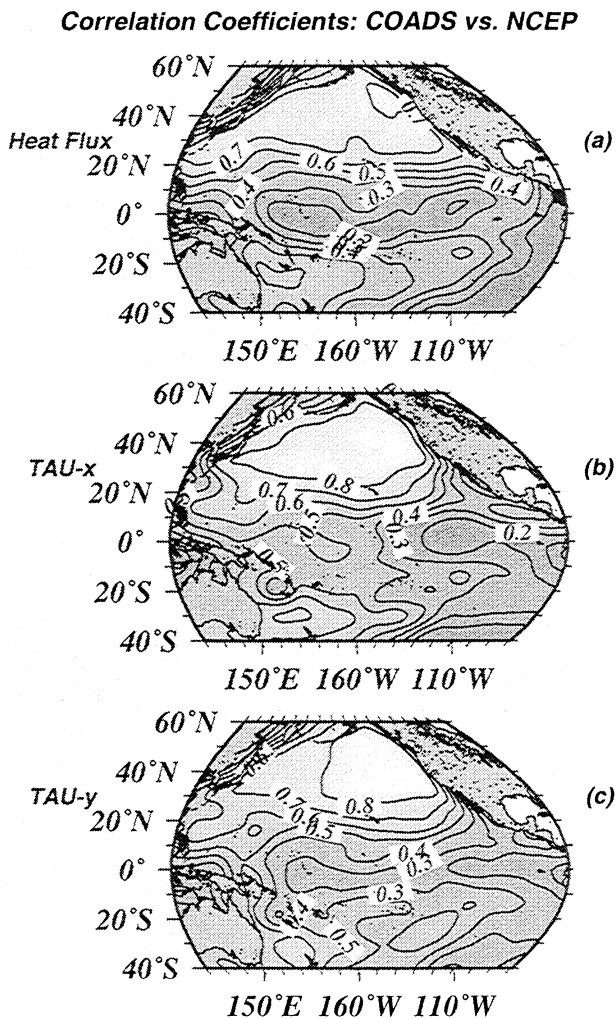


Figure 3. Correlation coefficients between the heat fluxes and wind stresses of the COADS/FSU and NCEP data sets. The spatially averaged confidence levels, based on the Davis [1976] autocorrelation timescale, are (top to bottom) 0.35, 0.33, and 0.36. The fields were smoothed with a 1000 km radius filter.

Figure 4 shows that the ratio of the standard deviations of the wind stress components is nearly unity outside the subtropical latitudes. Along the equator, COADS/FSU stresses are larger than NCEP stresses by a factor of up to 2.5 and 3.5 for the zonal and meridional components, respectively. The largest discrepancies again occur in the eastern tropics, which is an area with low density of observations in COADS/FSU and with little data assimilated into the NCEP model.

In order to discriminate among different frequency bands we computed cross spectra between the NCEP and COADS/FSU flux time series over the entire Pacific basin. We focus on El Niño/Southern Oscillation (ENSO) timescales (2–8 years) and decadal timescales (>8 years) as they are the target of many climate studies. Figure 5 shows the transfer function amplitudes and phases and the squared coherency for the zonal wind stress between the COADS/FSU and NCEP fields for these two period bands. For the coherent areas, such

as the central North Pacific, lags are smaller than ± 1 month for the ENSO band (a 4% error) and smaller than ± 3 months for the decadal band (a 3% error). It is important to note that the squared coherencies in Figure 5 have a spatial structure similar to the correlation maps of Figure 3. Over the basin the most coherent band is the ENSO band which has a typical squared coherence that greatly exceeds the 90% confidence level of 0.35 in the tropics from 120°W westward, in the western North Pacific north of 20°N, and in the western South Pacific middle latitudes. The eastern tropical Pacific remains problematic as insignificant coherencies are obtained for all interannual frequencies.

Similar results (not shown) are obtained for the meridional wind stress over the central North Pacific. Unlike the zonal stress coherencies, maximum coherencies in midlatitudes, for all frequencies, are located further east by 20°–30°, where anomalous winds associated with the Aleutian Low are oriented more meridionally. This also is a feature of the tropics where the eastern tropical Pacific shows some significant coherencies for the merid-

STANDARD DEVIATION RATIOS: COADS vs. NCEP

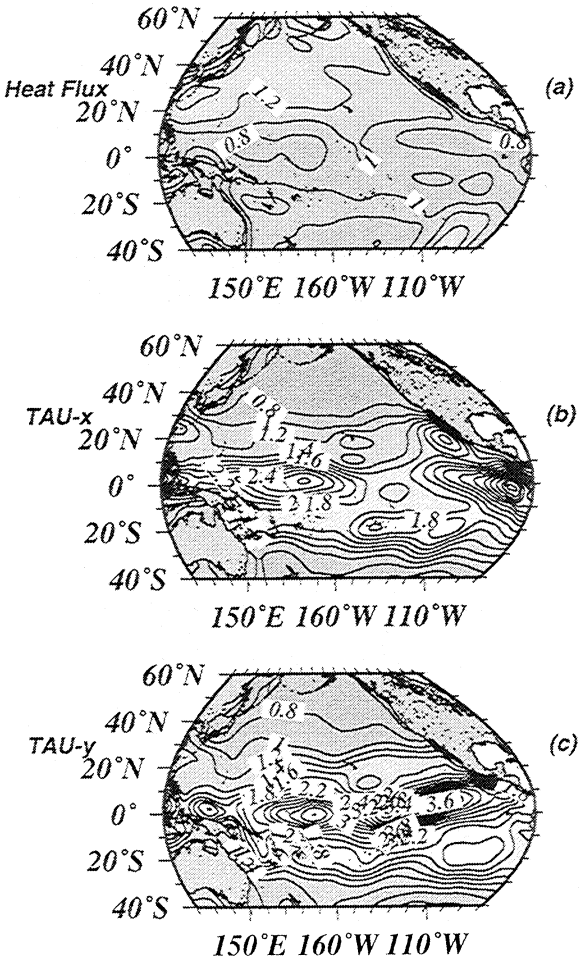


Figure 4. Ratios between the standard deviations of the heat fluxes and wind stresses of the COADS/FSU (numerator) and NCEP (denominator) data sets. The fields were smoothed with a 1000 km radius filter.

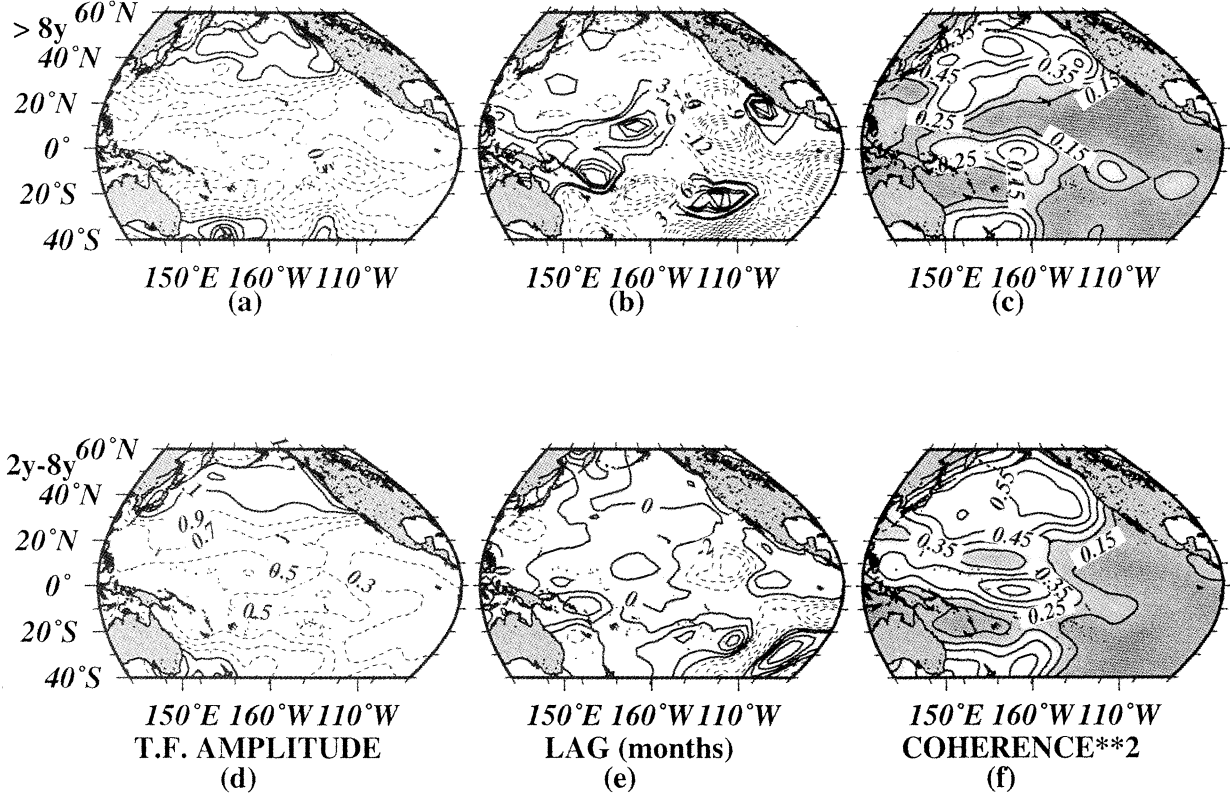


Figure 5. Cross spectral analysis between the COADS/FSU and NCEP zonal wind stresses. The three columns correspond to amplitude, phase and squared coherence of the transfer function. The labels on the left denote the frequency band in question, decadal and subdecadal (>8 year) and ENSO (2-8 years). The 40 year long time series was divided into four segments which overlapped 50%. The 90% confidence level is 0.35. The contour interval for squared coherences is 0.1 starting at 0.15 with contours <0.15 not plotted; the 0.35, 0.25 and 0.15 are included since most of them are parallel to the significant contours > 0.35. The contour intervals for transfer function amplitudes are 1.5, 1.3, 1.1, 0.9, 0.7, 0.5, etc. The contour interval for LAGS are 2 months for the ENSO band and 3 months for the decadal and subdecadal band. The transfer function amplitude is defined as NCEP over COADS.

ional component, unlike the zonal wind stress component.

For interseasonal frequencies (3, 6, and 9 month periods) both the zonal and meridional wind stresses are significantly coherent (not shown) only north of 20°N and show patterns similar to Figure 5. The transfer function amplitude indicates that NCEP wind stresses are roughly 10-30% smaller than COADS/FSU in the interseasonal band in that region.

3.2. Heat Fluxes

Table 2 shows some basic statistics between NCEP and COADS surface heat flux in seven key regions of the equatorial and North Pacific. Midlatitude areas exhibit a good correspondence in both amplitude and phase. As with the wind stress data, the major discrepancies are in the eastern and western equatorial Pacific areas (EEP and WEP areas). The NCEP heat flux in the EEP area (not shown) has an interdecadal oscillation which seems to be absent from the COADS record. It is interesting to note that in both data sets the maximum variability of heat fluxes (not shown) is observed

in the Kuroshio/Oyashio Extension area, a region which is crucial to decadal midlatitude ocean-atmosphere interactions [Nakamura *et al.*, 1997; Miller *et al.*, 1998; Deser *et al.* 1999; Qiu, 2000; Miller and Schneider, 2000].

Figure 3 (top) shows the correlation map of heat fluxes from NCEP and COADS. As with the wind stress correlations, minimum values are observed in the tropical band and increase toward higher latitudes. The Northern Hemisphere has larger correlations than the Southern Hemisphere while the maximum Southern Hemisphere correlations are seen off the Australian coast, most likely because of a higher sampling rate in this region.

Figure 4 (top) shows the standard deviation ratios of heat fluxes for COADS and NCEP. Unlike wind stresses, the ratios for heat fluxes in the tropical band are much closer to unity. In the midlatitude Northern Hemisphere the ratios are between 0.9 and 1.0. The RMS difference (not shown) in the tropics for $Q_C - Q_N$ is $O(5 \text{ W m}^{-2})$, while in the subtropical Northern Hemisphere it is $O(-5 \text{ to } -10 \text{ W m}^{-2})$. In the subtropical Southern

Table 2. Correlations, Standard Deviations ratios, Coherence, Amplitude of Transfer Function and Lag for COADS and NCEP surface heat fluxes

Area	Corr	SD	Coherence				
			2years	2.5years	3.3years	5years	10years
EEP	(0.33)	(0.96)	0.18	0.37	0.53	0.52	0.45
WEP	0.12	0.90	0.04	0.01	0.12	0.49	0.40
CCS	(0.86)	(1.10)	(0.65)	(0.69)	0.40	0.02	0.28
CNP	(0.81)	(1.26)	(0.64)	(0.77)	(0.73)	0.31	0.32
N 20°N	(0.66)	(1.16)	0.52	0.46	0.08	0.03	0.10
K.Ext.	(0.79)	(1.39)	0.57	(0.72)	0.32	0.12	0.16
WNP	(0.72)	(1.18)	0.33	(0.39)	0.52	(0.75)	(0.77)

CORR and SD were computed using anomalous time series with no filtering. Results from the cross-spectral analysis are shown for the five lowest (climate) bands of the computation (2, 2.5, 3.3, 5 and 10 years). All ratios are COADS/NCEP, and a negative lag implies that NCEP leads COADS. Values in parentheses are significant at the 90% level

Amplitude					Lag (months)				
2years	2.5years	3.3years	5years	10years	2years	2.5years	3.3years	5years	10years
0.34 (0.12)	0.54 (0.03)	0.79 (0.26)	0.83 (0.32)	0.79 (0.25)	-0.49 2.22	-0.52 11.2	2.31 -8.5	3.48 (-16.7)	-1.59 (-43.2)
(0.64) (0.75)	(0.68) (0.67)	0.08 0.31	0.27 0.60	(0.05) (-0.75)	(-1.36) (-0.75)	-1.81 (-0.75)	0.46 (-1.80)	5.16 (-4.52)	-9.98 10.06
(0.81) (0.83)	(0.41) (0.25)	0.31 0.13	0.19 0.19	-3.0 -3.34	-3.0 -3.34	-0.23 -0.23	-1.14 -0.67	-41.0 3.88	-41.0 -2.17
0.56 0.57	0.41 (0.51)	0.25 0.30	0.13 0.22	0.19 0.30	-1.41 -0.63	(-1.23) -1.64	-0.67 0.31	3.88 (0.81)	-41.0 (0.69)
0.53	0.61	0.97	(1.06)	(0.95)					

Hemisphere RMS differences are smaller than in the Northern Hemisphere and tend to zero on average in the band 20°S-40°S.

The cross-spectral analysis between NCEP and COADS heat fluxes is shown in Figure 6 for the ENSO (2-8 years) and decadal and subdecadal (>8 years) frequency bands. For regions where significant squared coherences are seen in the right the ratio of COADS over NCEP is less than unity for all frequencies. As with the wind stress comparison, errors in phase (Figure 6, middle) are small (no more than 4% to 5%). The sparsely sampled tropics and Southern Hemisphere do not show significant coherences. The most coherent areas are the western subtropical North Pacific and some highlatitude areas (Table 2). Similar to the analysis of wind stresses, the surface heat fluxes in the interseasonal bands (3 to 9 months) exhibit significant coherences (not shown) only north of 20°N, with COADS and NCEP heat fluxes having nearly the same amplitudes.

It is important to note that the shortwave fluxes from the NCEP reanalysis are known to be inaccurate and might contribute to errors in SST anomalies, especially during summer [Scott and Alexander, 1999]. In winter, however, the combined effect of the latent and sensible heat fluxes is larger than the shortwave by 1 order in midlatitudes [Cayan, 1992a]. In summer the midlatitude latent and sensible fluxes together are com-

parable to those of the shortwave fluxes so the shortwave flux errors can degrade the quality of ocean model summertime SST hindcasts. In the tropics, shortwave fluxes and the combined effect of sensible and latent heat fluxes are comparable year-round, but they normally act as a damping effect on SST anomalies in that region.

4. Ocean Model Response to COADS/FSU and NCEP forcing

4.1. OPYC Model

The primitive equation ocean model called the Ocean isoPYCnal (OPYC) model was developed by Oberhuber [1993] and applied by Miller et al. [1994, 1997, 1998], Cayan et al. [1995], and Auad et al. [1998a, 1998b] to study monthly through decadal-scale ocean variations over the Pacific Basin. Here an updated version of the model was used with higher resolution and a revised scheme for forcing with monthly mean fluxes.

The model is constructed with 10 isopycnal layers (each with nearly constant potential density but variable thickness, temperature, and salinity) that are fully coupled to a bulk surface mixed-layer model. The grid extends from 119°E to 70°W and from 67.5°S to 66°N, with periodic boundary conditions along the latitudes

of the Antarctic Circumpolar Current. The resolution is 1.5° in the midlatitude open ocean, with zonal resolution gradually increased to 0.65° resolution within a 10° band around the equator. Although the model is not eddy resolving, equatorial instability waves occur spontaneously, and eddies occur in the west wind drift of the midlatitudes. We only seek to study large-scale patterns in the response and regard this intrinsic variability as noise. The semi-implicit time step is 0.75 days.

Two versions of the surface forcing are employed: (1) monthly mean seasonal cycle fields plus monthly mean COADS/FSU anomalies and (2) monthly mean seasonal cycle fields plus monthly mean NCEP anomalies. The monthly mean seasonal cycle forcing is derived from various sources and is the same as used by *Miller et al.* [1994]. The monthly mean wind stress climatology is derived from a combination of monthly mean European Centre for medium-Range Weather Forecasts (ECMWF) midlatitude fields and monthly mean Hellerman-Rosenstein tropical climatology. The monthly mean seasonal cycle climatology of turbulent kinetic energy (TKE) input to the mixed layer is estimated from the same data sets [*Oberhuber*, 1993]. The surface freshwater flux is represented as a combination of observed monthly mean rainfall [*Legates and Willmott*, 1992], evaporation computed by bulk formula, plus a relaxation to the annual mean Levitus salinity field over 30-day timescales. The monthly mean seasonal cycle climatology of total surface heat flux is computed during spin-up (with no anomalous forcing) by determining

surface heat flux at each time step with bulk formulae that use evolving model SST with ECMWF-derived atmospheric fields (air temperature, humidity, cloudiness, etc.); the daily mean seasonal cycle of heat flux is then saved (averaged over the last 10 years of a 99-year spin-up) and subsequently used as specified forcing during the anomalously forced hindcasts.

Anomalous fields of monthly mean wind stress, total surface heat flux, and TKE are then added to the respective monthly mean seasonal cycles. Because there is no SST feedback to any of the anomalous forcing fields, the model is not constrained to reproduce the observed temperature variations (as could be achieved by adapting a *Haney* [1971] or *Barnier et al.* [1995] formulation). Because of the lack of data in the tropics we use the COADS/FSU blend wind stresses (and TKE estimates) as described in section 2. A similar strategy is employed by *Putman et al.* [2000] to improve the tropical wind stresses of the NCEP fields, but here we use the NCEP stresses in their original form. Specified surface freshwater flux anomalies are excluded from both hindcasts because of inadequate rainfall observations in COADS and unreliable precipitation estimates from the NCEP reanalysis [e.g., *Janowiak et al.*, 1998]. The continuous relaxation to annual mean Levitus salinity, however, implies that freshwater flux anomalies do occur in the hindcasts; however they have a weak influence on SST and mixed layer depth anomalies.

Near the equator the anomalous heat fluxes are poorly known because of the many gaps in ship weather reports. Moreover, tropical heat fluxes generally serve as

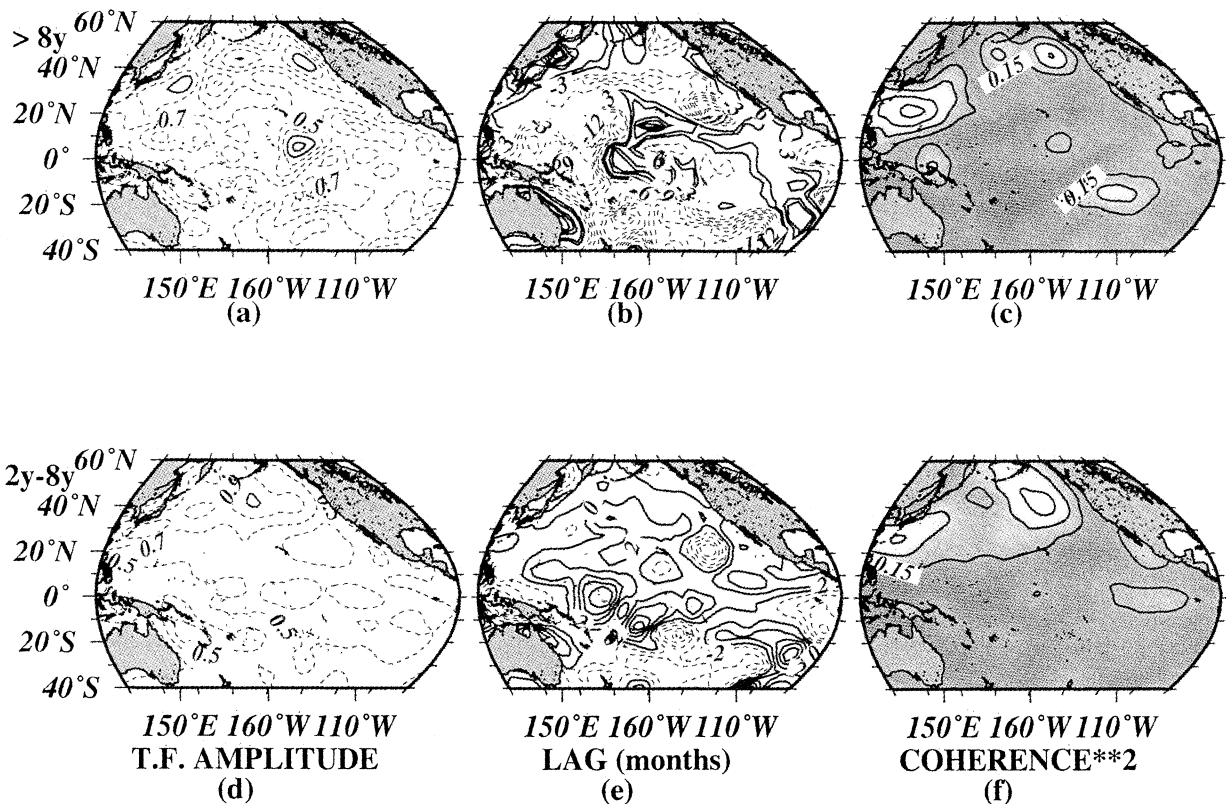


Figure 6. As in Figure 5 but for surface heat fluxes.

a damping mechanism [Liu and Gautier, 1990; Cayan, 1992b; Barnett et al., 1991], although Seager [1989] shows these fluxes can sometimes excite SST anomalies in certain locations. Therefore unless the wind-driven model SST reproduced the observed SST with nearly perfect fidelity, heat flux anomalies specified from observations would try to damp an SST anomaly that "was not there". This nonphysical forcing can then lead to an excitation of model SST anomalies with opposite sign as the observed. Hence a physically motivated Newtonian damping is employed within a 6° e-folding scale around the equator. The SST anomalies there are damped back to the model SST climatology (averaged from the last 10 years of the spin-up run) over timescales that depend on a damping coefficient divided by the mixed layer depth (following Miller et al. [1994]; see Barnett et al. [1991] for a map of the coefficient).

The monthly forcing strategy of Auad et al. [1998a, 1998b] is used to properly weight the monthly mean forcing anomalies, which are added to the seasonal cycle forcing, following Killworth [1996]. Miller et al. [1994] employ simple linear interpolation of the monthly mean forcing, which yields monthly mean model forcing that is typically weaker than the true monthly mean observed forcing. The Killworth [1996] scheme is a method for increasing the input monthly mean forcing fields to allow linear interpolation in time to yield correct monthly mean forcing.

The ocean model is run for two cases. The NCEP run (forced by anomalous NCEP fluxes) extends from January 1958 to December 1997. The COADS/FSU run (forced by anomalous COADS fluxes supplemented with FSU and reconstructed tropical stresses) extends from January 1951 to December 1997. Initial conditions for those runs are from the ninetieth year of the model spin-up with climatological forcing. Because there is no model SST feedback to the surface heat fluxes (except in a narrow equatorial band) there is a possibility of a drift in the model climatology because the model has not reached a complete equilibrium with mean flux forcing after 90–100 years of spin-up. The NCEP run (and a separate run with zero forcing anomalies) indeed exhibits a small and apparently inconsequential drift due to this effect. The COADS/FSU run, however, exhibits a larger drift in the model SST climatology.

Its origin appears to be mainly associated with COADS heat flux anomalies which have interdecadal variations that are not present in the NCEP heat fluxes. These interdecadal COADS heat flux anomalies are likely erroneously large because the "reduced thermal damping" effects of air-sea coupling should effectively shut off heat fluxes at very low-frequencies [e.g., Battisti et al., 1995; Barsugli and Battisti, 1998]. Attempts to remove these spurious trends and decadal variations a priori by trend removal and high-pass filtering [Kaylor, 1977] the COADS heat flux forcing fields fail to preserve the true low frequency variability in the forcing fields. So their effect is instead removed a posteriori

by computing the ocean model climatologies over three separate successive segments of the 1951–1997 run from which anomalies are then computed.

4.2. Modeled-Observed SST Comparisons

We next examine the performance of the two models runs, forced with NCEP and COADS/FSU anomalous forcing, in simulating SST observed in the COADS. The simple statistical analyses employed here include monthly mean anomalies for all months of the year and give a broad idea of the year-round model performance. A more detailed look at the model performance as a function of season, however, would show that winter month SST anomalies are much better simulated than summer months (as found by Miller et al. [1994]), mainly because of the strong forcing signals in winter and the high sensitivity of thin summer mixed layers to errors in the specified forcing.

Figure 7 shows the correlation coefficients between observed and modeled monthly mean SST anomalies for both runs. The patterns are fairly similar in that

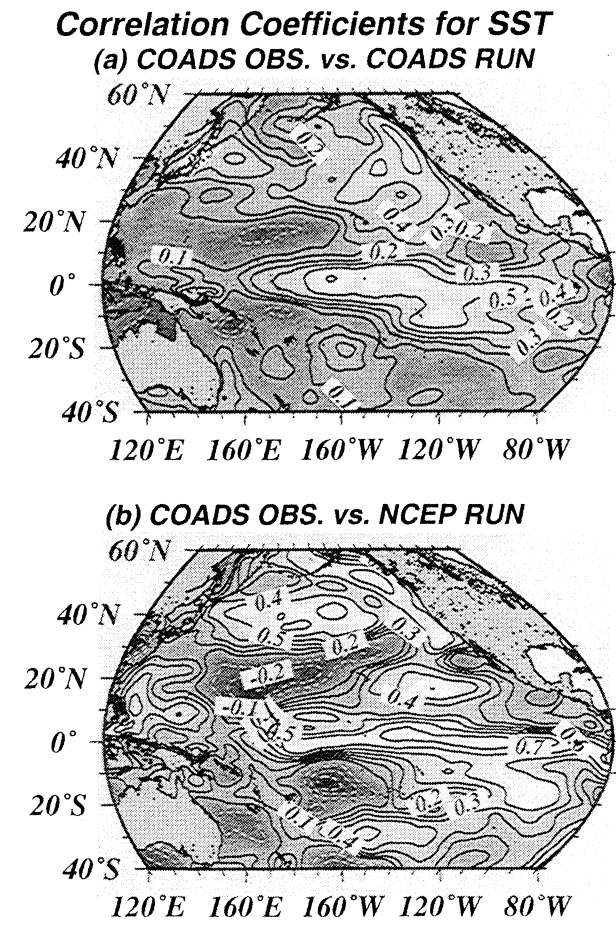


Figure 7. Correlation coefficients between observed SST (COADS) and model SST from the (top) COADS/FSU-forced run and from the (bottom) NCEP-forced run. The fields were smoothed with a 1000 km radius filter.

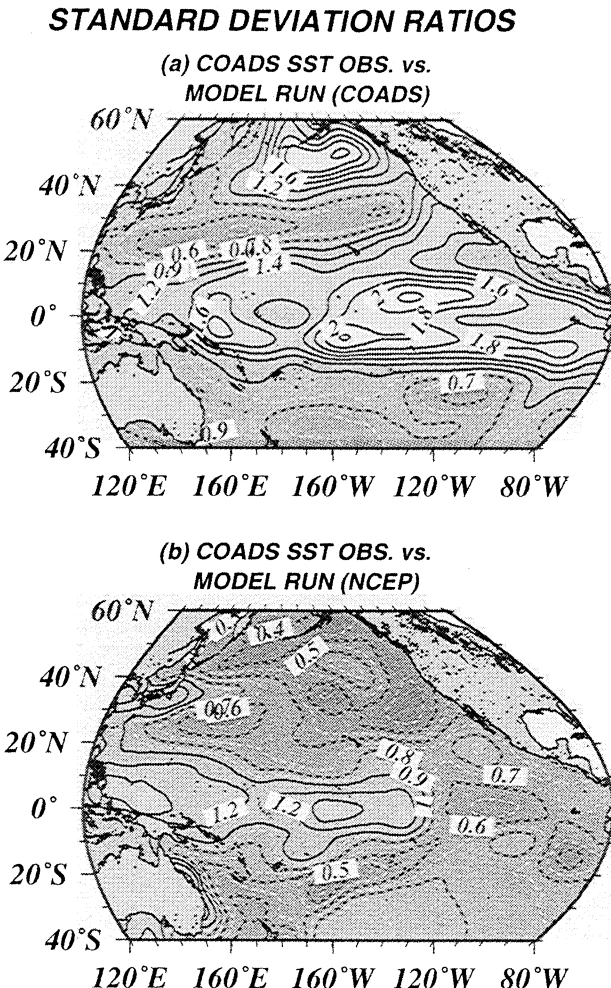


Figure 8. Ratios of the standard deviations between observations of SST anomalies from COADS (numerator) and the model SST anomalies (denominator) obtained from the (top) COADS/FSU-forced run and from the (bottom) NCEP-forced run. The fields were smoothed with a 1000 km radius filter.

they show the best correlations in the central and eastern tropical Pacific and the central and eastern midlatitude North Pacific north of 30°N. The South Pacific, where there are not as many observations of SST, wind stresses, and surface heat fluxes, exhibits much poorer correlations. The poor correlations seen in the western North Pacific, centered at 20°N between 160°E and 180°, also may be due to the lack of observations in that area. However, the model bulk mixed layer is very deep in that region (exceeding 150 m in winter) which was found, in separate model sensitivity experiments, to be due to the combined effects of Ekman downwelling and surface cooling during the entraining seasons [De Szoeke, 1980]. The excessively deep mixed layer may distribute the surface forcing too deep into the water column yielding poorer results.

The correlations between model and observed SST (Figure 7) for the COADS/FSU-forced run are lower

than those of *Miller et al.* [1994] and *Cayan et al.* [1995] because of several factors. This time interval is longer than the 1970–1988 period modeled in these previous studies and hence includes time periods with less confidently observed forcing and response fields. For example, the subset 1970–1988 winter midlatitude SST, from the previous model simulations, matches the correlations discussed by *Miller et al.* [1994] much more closely. However, the 1970–1988 year-round SST correlations are smaller than those of *Cayan et al.* [1995] in the midlatitudes, indicating the summer month periods are modeled here with less fidelity. This seems to be caused by the present model's previously mentioned tendency to produce eddies due to instabilities in the west wind drift. An ensemble of hindcast runs could drive down this eddy noise to better establish the forced part of the response, but that is beyond our computational means at this time.

The ratios of standard deviations (observed/model) for SST anomalies are shown in Figure 8. The COADS/FSU run tends to underestimate SST anomaly variance in the tropical Pacific and in the subpolar region of the North Pacific. The NCEP run overestimates SST anomaly variance throughout the Pacific except in a small region in the central equatorial Pacific. Both runs seriously overestimate SST anomaly variance in the subtropics of both hemispheres.

As was mentioned previously, errors in both the forcing and validating data may be large in these regions due to limited observations, and errors in the model may be large due to the large mean model mixed layer depth in this region.

A feature not evident in Figures 7 and 8 is that, on interannual timescales, the NCEP run produces El Niño and La Niña events that are roughly half the observed amplitude. This occurs in spite of the NCEP fluxes containing stronger than observed interseasonal variations. The weak interannual wind stresses of the NCEP analysis motivated *Putman et al.* [2000] to blend the FSU tropical stresses with the NCEP stresses to provide a more useful forcing dataset for future studies. COADS likewise suffers from weak interannual wind stress representation, hence motivating the use of a blended COADS/FSU wind-stress forcing dataset by *Miller et al.* [1994] and in this study.

4.3. Modeled-Observed Heat Storage Comparisons

We next examine the performance of the two models runs, forced with NCEP and COADS/FSU anomalous forcing, in simulating heat storage, here defined as ocean temperature integrated over the upper 400 m of the water column (scaled by density and heat capacity). Observed heat storage is taken from the *White* [1995] analysis of available subsurface temperature observations since 1955. *Chepurin and Carton* [1999] discuss potential deficits of this analysis. The simple statisti-

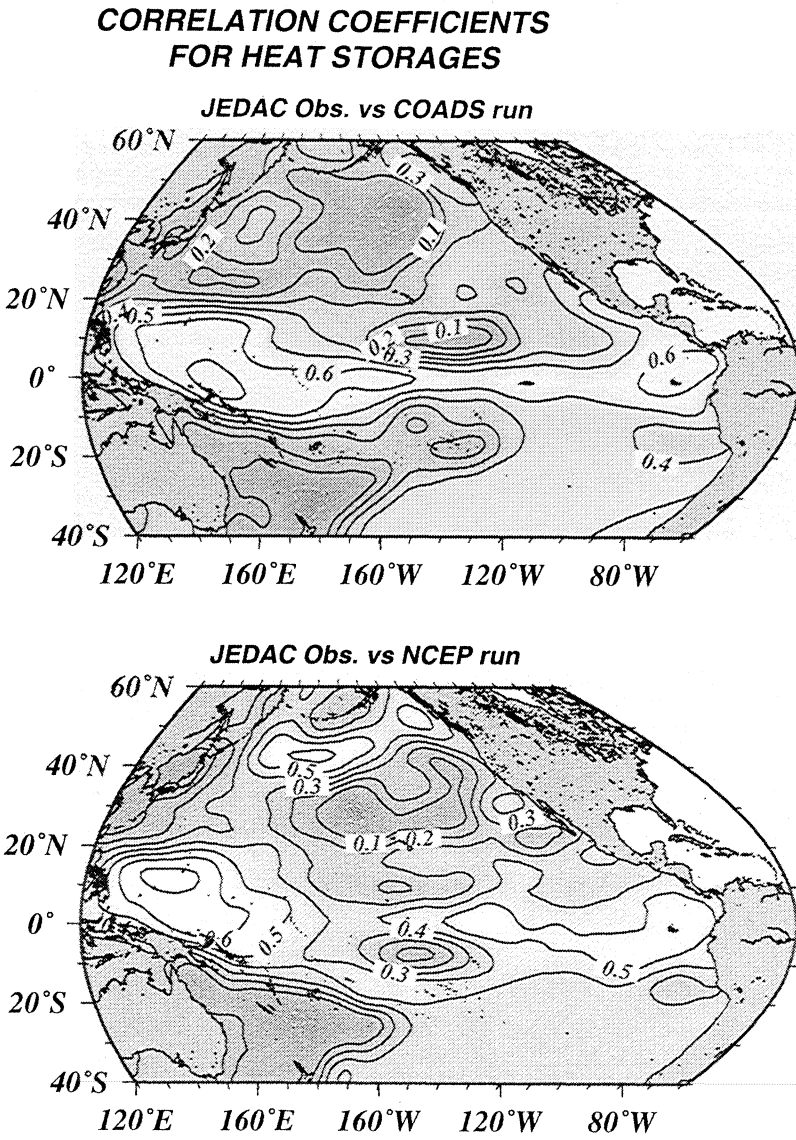


Figure 9. As in Figure 7 but for heat storages.

cal analyses here include monthly mean anomalies for all months of the year to give a synopsis of the year-round model performance. Heat storage includes components of response locally forced by diabatic processes (evidenced mainly as SST anomalies) and adiabatic processes (seen as thermocline heave) as discussed by Auad *et al.* [1998a,1998b]. Errors in the estimation of wind stress curl forcing, which largely controls the thermocline heave, may be large and may strongly influence the model response during periods of limited observations.

The correlations (zero time lag) between observed and modeled heat storage are shown in Figure 9. Maximum zero-lag correlations are obtained in the warm pool of the western tropical Pacific and in the eastern tropical Pacific. The NCEP run, unlike the COADS/FSU run, exhibits significant correlations for heat storage in the subpolar area, north of 40°N. The midlatitude regions of insignificant correlations cover a

much greater area than found by Auad *et al.* during the 1970-1988 time interval for heat storage on interannual and decadal timescales. Thus, the interseasonal variations of heat storage, which are inadequately simulated, appear to be dominating the correlation maps in Figure 9.

Figure 10 displays the ratios of standard deviations of heat storage (observations/model). Along the tropical strip, where significant correlations occurred in both runs, heat storage variance is nearly the same as observed in the western tropical Pacific but greater than observed in the eastern tropical Pacific. In the subpolar region, which showed significant correlations in the NCEP run, the model seriously overestimates the heat storage variability.

The model heat storage variations in the western tropical Pacific warm pool area are better correlated to observations than are SST variations. Since this region is dominated by local, rather than remote wind

forcing [Schneider *et al.* 1999], a reasonably accurate representation of the wind stress curl is responsible for the significant model-data correlations. However, wind stress curl from COADS/FSU and NCEP show surprisingly low correlations in the warm pool area even though simulated heat storages from both runs agree reasonably well with observations. It appears that a few energetic frequencies of the wind stress (associated with El Niño) in the western tropical and subtropical Pacific area drive the modeled fields that are responsible for this agreement with observed heat storage.

In the central North Pacific, model heat storage variations are poorly correlated with observations, while model SST anomalies are significantly correlated with observations. In this region, COADS and NCEP surface fluxes are also well correlated and directly force model SST anomalies through various processes [Miller *et al.*, 1994]. It is surprising to find that model heat storage response to these two correlated forcings does not match observations (except in the subpolar gyre for the NCEP run). Auad *et al.* [1998a,1998b] showed with an earlier version of this model that model thermocline dynamics are adequate to simulate heat storage fluctuations in midlatitudes that are significantly coherent with observations if one focuses on the interannual and interdecadal timescales. But that study was limited to

the time period 1970-1988, which has the highest density of subsurface data. Figure 9 shows low model-data heat storage correlation in midlatitudes occurs when including all climatic timescales from 1958-1997. The reasons for this include the intrinsic variability of the ocean model, sparse subsurface oceanic data before 1970, inaccurate wind stress curl forcing, and the inclusion of interseasonal timescales. Indeed, Figure 11 shows that the correlation between COADS and NCEP wind stress curl in the North Pacific is significant but does not exceed 0.7.

5. Summary and Discussion

A comparison of COADS (blended with tropical FSU wind stresses) and NCEP surface flux anomalies over the Pacific Ocean on climatic timescales from 1958-1997 was executed. The two data sets were then tested as forcing functions in separate simulations of Pacific Ocean variability using an ocean model.

Wind stress anomalies from the two data sets are well correlated in the midlatitude extratropics, more so in the highly sampled North Pacific than in the South Pacific. In the tropics and subtropics, low correlations were found between the two wind stress data sets; somewhat higher correlations occurred in the western part of these regions because of denser sampling than in the eastern part. The amplitudes of the stress variations of the two data sets are similar in midlatitudes. In the tropics, NCEP wind stresses are weaker than the COADS/FSU stresses, especially on interannual timescales, which is problematic for El Niño simulations.

Surface heat flux anomalies from the two data sets are well correlated on interannual and shorter timescales in the North Pacific Ocean north of 20°N, but they are poorly correlated elsewhere and on decadal timescales. In the extratropics the amplitudes of the heat flux variations of the two data sets are comparable, but in the tropics the NCEP heat fluxes are weaker than COADS.

Errors in the estimation of the COADS/FSU fluxes due to limited data sampling cannot be ruled out as the primary explanation for the low correlations found in this study. Indeed, areas with a high density of observations usually exhibit significant correlation between COADS/FSU and NCEP fluxes. This strongly suggests that data density controls the comparability and usefulness of the forcing fields. This idea is supported by a frequency domain analysis (including periods from 3 months to 10 years) that showed coherency is independent of frequency in the geographical areas where COADS/FSU and NCEP surface fluxes are significantly correlated.

Ocean simulations were then used to test the sensitivity of the oceanic response to the two different forcing data sets. One simulation used the surface flux anomalies specified from NCEP (1958-1997), and the other used those of COADS/FSU (1951-1997).

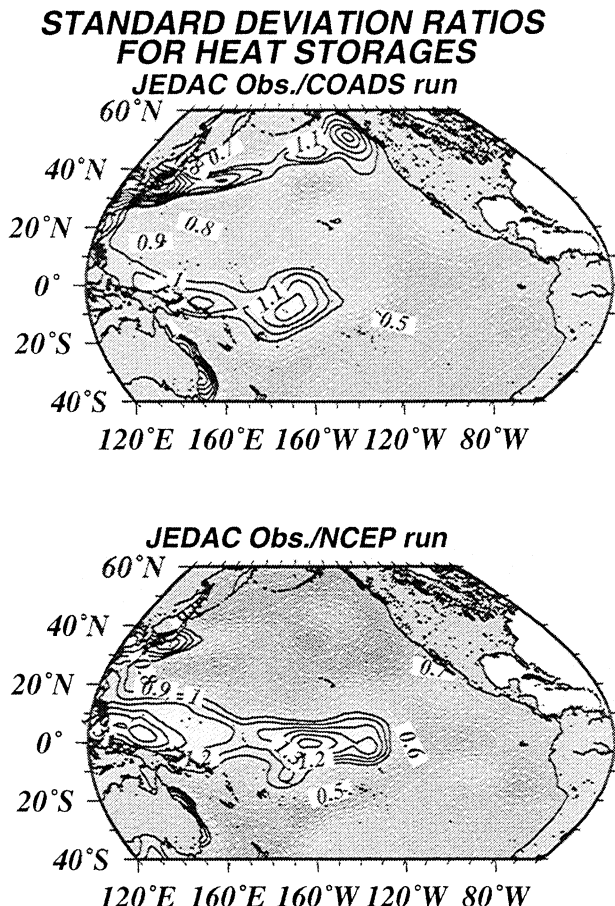


Figure 10. As in Figure 8 but for heat storages.

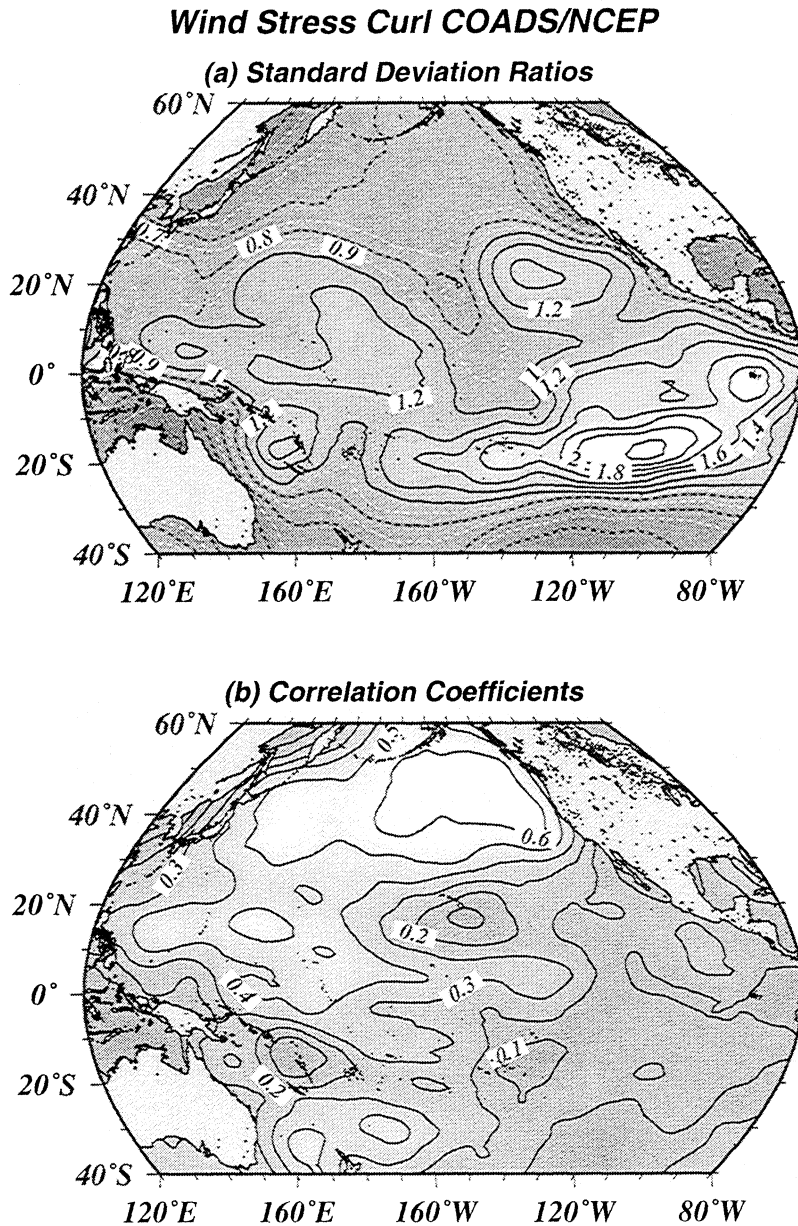


Figure 11. Wind stress curl comparison. (top) standard deviation ratios of COADS/FSU to NCEP wind stress curls and (bottom) correlation coefficients. The fields were smoothed with a 1000 km radius filter.

The midlatitude SST hindcasts were superior when using the NCEP fluxes, suggesting that the NCEP data are eminently suitable for ocean hindcast process studies in those regions. Tropical SST anomalies had similar skill levels for the two hindcasts when considering all climatic timescales. However, on interannual timescales the NCEP tropical wind stresses are weaker than COADS/FSU stresses, consequently yielding interannual tropical SST anomalies that are much weaker than observed. Adjusting NCEP tropical wind stresses to alleviate this problem is presently the most feasible strategy, as *Putnam et al.* [2000] showed using FSU stresses.

Heat storage anomalies in the two simulations were also compared with observations. Significant correla-

tions of modeled and observed tropical heat storage variations including all climatic timescales were found for both hindcasts. However, only the NCEP simulation exhibited significant correlations with observed midlatitude heat storage, and that was limited to a portion of the North Pacific subpolar gyre and eastern boundary. Since COADS and NCEP fluxes were correlated ($r=0.7$) in this same region, minor differences in the two forcing functions sets can lead to substantially different model ocean heat storage responses. The main discrepancy between modeled and observed heat storage can be traced to inadequate correlation ($r=0.5$) between NCEP and COADS wind stress curl anomalies which dominate the driving of thermocline variations in the subpolar North Pacific [*Auad et al.*, 1998a, 1998b; *Miller et al.*, 1998;

[Deser *et al.*, 1999]. Apparently, the consistent dynamics of the NCEP reanalysis model efficiently organizes the input observations to yield a better estimate of wind stress curl than is obtainable from COADS observations alone.

Problems arise in explaining decadal-scale COADS heat flux variations and in removing their potential effects on ocean model response. Some of the fundamental COADS marine weather observations (wind speed, SST, etc.) that are used to estimate the surface fluxes are known to contain suspicious low-frequency variability due to changes in observational procedures, ship characteristics, and instrumentation [Michaud and Lin, 1992; The main discrepancy between modeled and observed heat storage can be traced to inadequate correlation ($r=0.5$) between NCEP and COADS wind stress curl anomalies which dominate the driving of thermocline variations in the subpolar North Pacific [Auad *et al.*, 1998a,b; Miller *et al.*, 1998; Deser *et al.*, 1999]. Apparently the consistent dynamics of the NCEP reanalysis model efficiently organizes the input observations to yield a better estimate of wind stress curl than is obtainable from COADS observations alone.

Problems arise in explaining decadal-scale COADS heat flux variations and in removing their potential effects on ocean model response. Some of the fundamental COADS marine weather observations (wind speed, SST, etc.) that are used to estimate the surface fluxes are known to contain suspicious low frequency variability due to changes in observational procedures, ship characteristics, instrumentation [Michaud and Lin, 1992; Ward and Hoskins, 1996]. The NCEP decadal-scale heat fluxes had much smaller amplitude than those of COADS which is consistent with what is anticipated from coupled ocean-atmosphere model studies [Barsugli and Battisti, 1998; Bhatt *et al.*, 1998].

The results of this study suggest that the NCEP surface fluxes overall yielded a better basinwide ocean hindcast than the COADS/FSU fluxes, except for the serious problems with weak interannual variability in the tropics. Denser and more frequent observations of surface variables for deriving air-sea fluxes are therefore needed in many key areas of the Pacific Ocean, especially the eastern tropical Pacific and the western subtropical Pacific. These data can then be used in atmospheric analyses to derive consistent long-term forcing functions for testing ocean models and diagnosing climate variations. Sustained basin-scale long-term observing programs using new techniques of remote sensing and in situ measurements, such as planned under the the Pacific Basinwide Extended Climate Study, are the best strategy for achieving this goal.

Acknowledgments.

This research is funded in part by the National Oceanic Atmospheric Administration, U.S. Department of Commerce, under grants NA77RJ0453 (Experimental Climate Prediction Center), NA47GP0188 (Consortium for Ocean's Role in Climate), NA66GP0274 (Paleoclimate Program), by the Na-

tional Science Foundation under grants OCE97-11265 and OCE00-82543, and by the National Aeronautics and Space Administration under grant NAG5-8292. The views expressed herein are those of the authors and do not necessarily reflect the views of NOAA or any of its sub-agencies. We are grateful to Warren White for providing us with the JEDAC dataset of subsurface temperature observations that made the modeled-observed heat storage comparisons possible. We thank Emelia Bainto for her valuable technical support. Josef Oberhuber generously provided modeling advice and access to his latest codes, for which we are grateful. Many important suggestions that greatly improved the manuscript were provided in detailed reviews by Mike Alexander, an anonymous referee, and Mike Spall.

References

- Auad, G., A. J. Miller, and W. B. White, Simulation of heat storages and associated heat budgets in the Pacific Ocean, 1, El Niño-Southern Oscillation timescale, *J. Geophys. Res.*, 103, 27,603-27,620, 1998a.
- Auad, G., A. J. Miller, and W. B. White, Simulation of heat storages and associated heat budgets in the Pacific Ocean, 2, Interdecadal timescale, *J. Geophys. Res.*, 103, 27,621-27,635, 1998b.
- Barnett, T. P., Long-term trends in surface temperature over the oceans, *Mon. Weather Rev.*, 112, 303-312, 1984.
- Barnett, T. P., M. Latif, E. Kirk, and E. Roeckner, On ENSO physics, *J. Clim.*, 4, 487-515, 1991.
- Barnier, B., L. Siefridt, and P. Marchesiello, Thermal forcing for a global ocean circulation model using a 3-year climatology of ECMWF analysis, *J. Mar. Syst.*, 6, 363-380, 1995.
- Barsugli, J. J., and D. S. Battisti, The basic effects of atmosphere-ocean thermal coupling on midlatitude variability, *J. Atmos. Sci.*, 55, 477-493, 1998.
- Battisti, D. S., U. S. Bhatt, and M. A. Alexander, A modeling study of the interannual variability in the wintertime North Atlantic Ocean, *J. Clim.*, 8, 3067-3083, 1995.
- Bennett, A. F., B. S Chua, D. E. Harrison, and M. J. McPhaden, Generalized inversion of tropical Atmosphere-Ocean data and a coupled model of the tropical Pacific, *J. Clim.*, 11, 1768-1792, 1998.
- Bennett, A. F., B. S Chua, D. E. Harrison, and M. J. McPhaden, Generalized inversion of Tropical Atmosphere-Ocean (TAO) data and a coupled model of the tropical Pacific, part II,: The 1995-96 La Niña and 1997-98 El Niño, *J. Clim.*, 13, 2770-2785, 2000.
- Betts, A. K., S. Y. Hong, and H. L. Pan, Comparison of NCEP-NCAR reanalysis with 1987 FIFE data, *Mon. Weather Rev.*, 124, 1480-1498, 1996.
- Bhatt, U. S., M. A. Alexander, D. S. Battisti, D. D. Houghton, and L. M. Keller, Atmosphere-ocean interaction in the North Atlantic: Near-surface climate variability, *J. Clim.*, 11, 1615-1632, 1998.
- Blanc, T. V., Variation of bulk-derived surface flux, stability, and roughness results due to the use of different transfer coefficient schemes, *M. J. Phys. Oceanogr.* 15, 650-669, 1985.
- Bony, S., Y. Sud, K. M. Lau, J. Susskind, and S. Saha, Comparison and satellite assessment of NASA/DAO and NCEP-NCAR reanalyses over tropical ocean: Atmospheric hydrology and radiation, *J. Clim.*, 10, 1441-1462, 1997.
- Cayan, D. R., Variability of latent and sensible heat fluxes estimated using bulk formulae, *Atmos. Ocean*, 30, 1-42, 1992a.
- Cayan, D. R., Latent and sensible heat flux anomalies over the northern oceans: Driving the sea surface temperature, *J. Phys. Oceanogr.*, 22, 859-881, 1992b.

- Cayan, D. R., A. J. Miller, T. P. Barnett, N. E. Graham, J. N. Ritchie, and J. M. Oberhuber, Seasonal-interannual fluctuations in surface temperature over the Pacific: Effects of monthly winds and heat fluxes, in *Natural Climate Variability on Decadal-to-Century Time Scales*, 133-150 pp., edited by Nat. Acad. Press, Washington, D.C., 133-150, 1995.
- Chepurin, G. A., and J. A. Carton, Comparison of retrospective analyses of the global ocean heat content, *Dyn. Atmos. Oceans*, 29, 119-145, 1999.
- da Silva, A. M., C. C. Young, and S. Levitus, *Atlas of Surface Marine Data*, Vol. 3, *Anomalies of Heat and Momentum Fluxes*, NOAA Atlas Ser., NESDIS 7, Natl. Oceanic and Atmos. Admin., Washington, D.C., 413 pp., 1994.
- Davis, R. E., Predictability of sea surface temperature and sea level pressure anomalies over the North Pacific Ocean, *J. Phys. Oceanogr.*, 6, 249-266, 1976.
- Deser, C., M. A. Alexander, and M. S. Timlin, Evidence for a wind-driven intensification of the Kuroshio Current Extension from the 1970s to the 1980s, *J. Clim.*, 12, 1697-1706, 1999.
- De Szoeke, R. A., On the effects of horizontal variability of wind stress on the dynamics of the ocean mixed layer, *J. Phys. Oceanogr.*, 10, 1439-1454, 1980.
- Fevrier, S., C. Frankignoul, J. Sirven, M. K. Davey, P. Delecluse, S. Ineson, J. Macias, N. Sennechael, and D. B. Stephenson, A multivariate intercomparison between three oceanic GCMs using observed current and thermocline depth anomalies in the tropical Pacific during 1985-1992, *J. Mar. Syst.*, 24, 249-275, 2000.
- Frankignoul, C., C. Duchene, and M. A. Cane, A statistical approach to testing equatorial ocean models with observed data, *J. Phys. Oceanogr.*, 19, 1191-1207, 1989.
- Frankignoul, C., S. Fevrier, N. Sennechael, J. Verbeek, and P. Braconnat, An intercomparison between four tropical ocean models - Thermocline variability, *Tellus*, 47, 351-364, 1995.
- Giese, B. S., and J. A. Carton, Interannual and decadal variability in the tropical and midlatitude Pacific, *J. Clim.*, 12, 3402-3418, 1999.
- Goldenberg, S. B., and J. J. O'Brien, Time and space variability of tropical Pacific wind stress, *Mon. Wea. Rev.*, 109, 1190-1207, 1981.
- Halliwell, G. R., Simulation of North Atlantic decadal and multidecadal winter SST anomalies driven by basin-scale atmospheric circulation anomalies, *J. Phys. Oceanogr.*, 28, 5-21, 1998.
- Haney, R. L., Surface thermal boundary condition for ocean circulation models, *J. Phys. Oceanogr.*, 1, 241-248, 1971.
- Harrison, D. E., B. S. Giese, and E. S. Sarachick, Mechanisms of SST change in the equatorial wave-guide during the 1982-83 ENSO, *J. Clim.*, 3, 173-188, 1990.
- Isemer, H., and L. Hasse, *The Bunker Climate Atlas of the North Atlantic Ocean*, Vol. 2, *Air-sea interactions*, Springer Verlag, New York, 1987.
- Iwasaka, N., and J.M. Wallace, Large-scale air-sea interaction in the Northern Hemisphere from a view point of variations of surface heat flux by SVD analysis, *J. Meteorol. Soc. Jpn.*, 11, 781-794, 1995.
- Janowiak, J. E., A. Gruber, C. R. Kondragunta, R. E. Livezey, and G. J. Huffman, A comparison of the NCEP-NCAR reanalysis precipitation and the GPCC rain gauge-satellite combined dataset with observational error considerations, *J. Clim.*, 11, 2960-2979, 1998.
- Kalnay, E., et al., The NMC/NCAR reanalysis project, *Bull. Am. Meteorol. Soc.*, 77, 437-471, 1996.
- Kaylor, R. E., Filtering and decimation of digital time series, *Tech. Rep. BN 850*, 42 pp., Inst. for Phys. Sc. and Technol., Univ. of Md., 42 pp., 1977.
- Killworth, P., Time interpolation of forcing fields in ocean models, *J. Phys. Oceanogr.*, 4, 136-143, 1996.
- Kleeman, R., R. A. Colman, N. R. Smith, and S. B. Power, A recent change in the mean state of the Pacific basin climate: Observational evidence and atmospheric and oceanic responses, *J. Geophys. Res.*, 101, 20,483-20,499, 1996.
- Legates, D. R., and C. J. Willmott, A comparison of GCM-simulated and observed mean January and July precipitation, *Global Planet. Change*, 97, 345-363, 1992.
- Liu, W. T., and C. Gautier, Thermal forcing on the tropical Pacific from satellite data, *J. Geophys. Res.*, 95, 13,209-13,217, 1990.
- Luksch, U. and H. V. Storch, Modeling the low-frequency sea surface temperature variability in the North Pacific, *J. Clim.*, 5, 893-906, 1992.
- Lysne, J., P. Chang, and B. Giese, Impact of the extratropical Pacific on equatorial variability, *Geophys. Res. Lett.*, 24, 2589-2592, 1997.
- Marshall, G. J., and S. A. Harangozo, An appraisal of NCEP/NCAR reanalysis MSLP data viability for climate studies in the South Pacific, *Geophys. Res. Lett.*, 27, 3057-3060, 2000.
- Michaud, R., and C. A. Lin, Monthly summaries of merchant ship surface marine observations and implications for climate variability studies, *Clim. Dyn.*, 7, 45-55, 1992.
- Miller, A. J., and N. Schneider, Interdecadal climate regime dynamics in the North Pacific Ocean: Theories, observations and ecosystem impacts, *Progr. Oceanogr.*, 47, 355-379, 2000.
- Miller, A. J., T. P. Barnett, and N. E. Graham, A comparison of some tropical ocean models - Hindcast skill and El Niño evolution, *J. Phys. Oceanogr.*, 23, 1567-1591, 1993.
- Miller, A. J., D. R. Cayan, T. P. Barnett, N. E. Graham, and J. M. Oberhuber, Interdecadal variability of the Pacific Ocean: Model response to observed heat flux and wind stress anomalies, *Clim. Dyn.*, 9, 287-302, 1994.
- Miller, A. J., W. B. White, and D. R. Cayan, North Pacific thermocline variations on ENSO time scales, *J. Phys. Oceanogr.*, 27, 2023-2039, 1997.
- Miller, A. J., D. R. Cayan, and W. B. White, A westward-intensified decadal change in the North Pacific thermocline and gyre-scale circulation, *J. Clim.*, 11, 3112-3127, 1998.
- Morrissey, M. L., An evaluation of ship data in the equatorial western Pacific, *J. Clim.*, 3, 99-112, 1990.
- Nakamura, H., G. Lin, and T. Yamagata, Decadal climate variability in the North Pacific during the recent decades, *Bull. Am. Meteorol. Soc.*, 78, 2215-2225, 1997.
- Oberhuber, J. M., Simulation of the Atlantic circulation with a coupled sea ice - Mixed layer isopycnal general circulation model, part I, Model description, *J. Phys. Oceanogr.*, 23, 808-829, 1993.
- Parrish, R. H., F. B. Schwing, and R. Mendelsohn, Mid-latitude wind stress: The energy source of climatic shifts in the North Pacific Ocean, *Fish. Oceanogr.*, 9, 224-238, 2000.
- Pavia, E., and J. J. O'Brien, Weibull statistics of wind speed over the ocean, *J. Clim. Appl. Meteorol.*, 25, 1324-1332, 1986.
- Putman, W. M., D. M. Legler, and J. J. O'Brien, Interannual variability of synthesized FSU and NCEP-NCAR reanalysis pseudostress products over the Pacific Ocean, *J. Clim.*, 13, 3003-3016, 2000.
- Qiu, B., Interannual variability of the Kuroshio Extension system and its impact on the wintertime SST field, *J. Phys. Oceanogr.*, 30, 1486-1502, 2000.
- Ramage, C. S., Can shipboard measurements reveal secular

- changes in air-sea heat flux?, *J. Clim. Appl. Meteorol.*, **23**, 187-193, 1984.
- Ramage, C. S., Secular changes in reported surface winds over the oceans, *J. Clim. Appl. Meteorol.*, **26**, 525-528, 1987.
- Schneider, N., S. Venzke, A. J. Miller, D. W. Pierce, T. P. Barnett, C. Deser, and M. Latif, Pacific thermocline bridge revisited, *Geophys. Res. Lett.*, **26**, 1329-1332, 1999.
- Scott, J. D., and M. A. Alexander, Net shortwave fluxes over the ocean, *J. Phys. Oceanogr.*, **29**, 3167-3174, 1999.
- Seager, R., Modeling tropical Pacific sea-surface temperature - 1970-87, *J. Phys. Oceanogr.*, **19**, 419-434, 1989.
- Seager, R., Y. Kushnir, M. Visbeck, N. Naik, J. Miller, G. Kralmann, and H. Cullen, Causes of Atlantic Ocean climate variability between 1958 and 1998, *J. Clim.*, **13**, 2845-2861, 2000.
- Sennechael, N., C. Frankignoul, and M. A. Cane, An adaptive procedure for tuning a sea surface temperature model, *J. Phys. Oceanogr.*, **24**, 2288-2305, 1994.
- Stockdale, T. N., A. J. Busalacchi, D. E. Harrison, and R. Seager, Ocean modeling for ENSO, *J. Geophys. Res.*, **103**, 14,325-14,355, 1998.
- Tanimoto, Y., N. Iwasaka, and K. Hanawa, Relationships between sea surface temperature, the atmospheric circulation and air-sea fluxes on multiple time scales, *J. Meteorol. Soc. Jpn.*, **75**, 831-849, 1997.
- Taylor, P. K., The determination of surface fluxes of heat and water by satellite microwave radiometry and in situ measurements, in *Large-scale Oceanographic Experiments and Satellites*, edited by C. Gautier and M. Fieux, D. Reidel, *NATO ASI Series C*, Sciences, vol. 128 pp., 223-246, 1984.
- Trenberth, K. E., and C. J. Guillemot, Evaluation of the atmospheric moisture and hydrological cycle in the NCEP/NCAR reanalyses, *Clim. Dyn.*, **14**, 213-231, 1998.
- Trenberth, K.E., and J.W. Hurrell, Decadal atmosphere-ocean variations in the Pacific, *Clim. Dyn.*, **9**, 303-319, 1994.
- Waliser, D. E., Z. Shi, J. R. Lanzante, and A. H. Oort, The Hadley circulation: Assessing NCEP/NCAR reanalysis and sparse in situ estimates, *Clim. Dyn.*, **15**, 719-735, 1999.
- Ward, M. N., and B. J. Hoskins, Near-surface wind over the Global Ocean 1949-1988, *J. Clim.*, **9**, 1877-1895, 1996.
- Weare, B. C., Uncertainties in estimates of surface heat fluxes derived from marine reports over tropical and subtropical oceans, *Tellus*, **41**, 357-370, 1989.
- Weare, B. C., Comparison of NCEP-NCAR cloud radiative forcing reanalyses with observations, *J. Clim.*, **10**, 2200-2209, 1997.
- White, W. B., Design of a global observing system for gyre-scale upper ocean temperature variability, *Prog. Oceanogr.*, **36**, 169-217, 1995.
- Woodruff, S. D., R. J. Slutz, R. L. Jenne, and P. M. Steurer, A comprehensive ocean-atmosphere data set, *Bull. Am. Meteorol. Soc.*, **68**, 1239-1250, 1987.
- Wright, P. B., Problems in the use of ship observations for the study of interdecadal climate changes, *Mon. Weather Rev.*, **114**, 1028-1034, 1986.
- Xie, S. P., T. Kunitani, A. Kubokawa, M. Nonaka, and S. Hosoda, Interdecadal thermocline variability in the North Pacific for 1958-1997: A GCM simulation, *J. Phys. Oceanogr.*, **30**, 2798-2813, 2000.
- Yang, S. K., Y. T. Hou, A. J. Miller, and K. A. Campana, Evaluation of the earth radiation budget in NCEP-NCAR reanalysis with ERBE, *J. Clim.*, **12**, 477-493, 1999.

G. Auad, D. Cayan, A. Miller, and J. Roads, Climate Research Division, Scripps Institution of Oceanography, La Jolla, CA, 92093. (e-mail: guillo@ucsd.edu; dcayan@ucsd.edu; ajmiller@ucsd.edu; jroads@ucsd.edu)

(Received January 28, 2000; revised January 17, 2001; accepted January 18, 2001.)